

EREM 78/4

Journal of Environmental Research,
Engineering and Management
Vol. 78 / No. 4 / 2022
pp. 121–136
DOI 10.5755/j01.erem.78.4.31243

**Three-dimensional Numerical Evaluation of Hydraulic Efficiency and
Discharge Coefficient in Gate Inlets**

Received 2022/04

Accepted after revision 2022/10


<http://dx.doi.org/10.5755/j01.erem.78.4.31243>

Three-dimensional Numerical Evaluation of Hydraulic Efficiency and Discharge Coefficient in Gate Inlets

Melquisedec Cortés Zambrano*, **Helmer Edgardo Monroy González,**
Wilson Enrique Amaya Tequia

Faculty of Civil Engineering, Santo Tomas Tunja University. Address Av. Universitaria No. 45-202.
Tunja – Boyacá - Colombia

*Corresponding author: melquisedec.cortes@usantoto.edu.co

Floods are one of the causes of ground movement and displacement, and due to rapid urbanization and urban growth may occur more frequently than before. The characteristics of an urban drainage system can define the occurrence and extent of flooding, where catchment elements have a determining role. This document presents the numerical investigation of the hydraulic inlet efficiency and the discharge coefficient of seven types of grate inlets. The FLOW-3D® simulator is used to test the gratings at a full scale, under flow rates of $Q = 24, 34.1, 44, 100, 200$ and 300 L/s, preserving the configuration of the experimental prototype with longitudinal slopes of 1.0%, 1.5% and 2.0% and a fixed cross slope, for a total of 126 models. Based on the results, hydraulic inlet efficiency curves and discharge coefficients are constructed for each type and a longitudinal slope condition. The results are adjusted with empirical formulations proposed in other investigations, serving to verify the results of physical testing of prototypes.

Keywords: grate inlet, inlet efficiency, discharge coefficient, computational fluid dynamic, 3D modelling.

Introduction

Floods are one of the causes of displacement (World Bank, 2019) that are accentuated by rapid urbanization and population growth in cities (UNDRR and CRED, 2018). The drainage network plays a fundamental role in protecting urban activities in cities (Cosco et

al., 2020). The functionality of catchment structures, such as drains, can define the occurrence and extent of urban flooding due to rain (Jang et al., 2019; Leitão et al., 2017). These elements are often overlooked and may not be considered in drainage models (Kleidorfer

et al., 2018); as such, they have become weaknesses in the design and management of infrastructure (Sedano-Cruz et al., 2013), even when the underlying system has sufficient capacity (Palla et al., 2018).

This has increased the pressure to find solutions to the problems of storm water runoff (Faram and Harwood, 2002), as an integrated numerical approximation of the processes involved are sought (Aragón-Hernández, 2013; Ellis and Marsalek, 1996). Several numerical and physical approaches have been developed, in order to determine the hydraulic efficiency of the catchment structures, understand the variables that intervene in their hydraulic behavior (Carvalho et al., 2019), improve the response to different events (Yazdanfar and Sharma, 2015), and mitigate the effects of floods (Téllez-Álvarez et al., 2020).

Although scale models are one of the study options, Argue and Pezzaniti (1996) found that the reduction of scale can cause errors. Thus, there is a growing interest in the comparison of results between scaled down and full-scale models. This demonstrates the importance of assuming physical modelling and numerical modelling to be complementary approaches (Antunes do Carmo, 2020).

For this reason, numerical modelling has been used as a procedure to verify the efficiency of sewer elements. The predictions of computational fluid dynamics (CFD) have been demonstrated to adequately reproduce the hydraulic characteristics of operation. The volume of fluid (VOF) begins to have a relevant role in the investigation and prediction of open channel flow (Khazaei and Mohammadiun, 2010) as an element to represent the complete biphasic three-dimensional fluid dynamics.

Kaushal et al. (2012) and Mohsin and Kaushal (2016) have validated and optimized hydraulic processes with inverted traps, in which the results adequately describe the surface conditions of free water, velocity and static pressure for a variable flow as well as geometric parameters that resemble the experimental conditions, allowing us to determine the efficiencies of these hydraulic structures.

Ghanbari and Heidarnejad (2020) have simulated the three-dimensional flow field over the piano key weirs to study the flow hydraulics and compare the discharge rates. They have investigated the effect of each model and its discharge coefficient. Their results suggested that the data from the numerical model were adequately consistent with those from the laboratory model.

The results obtained by Tellez-Alvarez et al. (2003), Gómez Valentin (2007), Fang et al. (2010), Russo (2010), Gómez et al. (2016), Lopes et al. (2016), Téllez Álvarez et al. (2017) and Tellez-Alvarez et al. (2019, Chapter 65) have demonstrated the abilities of three-dimensional computational fluid dynamics as a virtual laboratory to evaluate and verify the efficiency in the interception of inflow in drains in different configurations. This has allowed computational fluid dynamic simulation to be converted into a technical support and development tool (Faram and Harwood, 2000).

The objective of this research is to study the catchment capacity of grate inlets through a three-dimensional (3D) numerical hydrodynamic approach that would allow the evaluation of the hydraulic efficiency and discharge coefficient of some types of grates. This is carried out by means of the implementation of FLOW-3D® (Flow Science, 2019), a CFD numerical model based on the VOF method. In addition, we also sought to verify the results of the physical experimental phase of prototypes previously developed by Chaparro Andrade and Abaunza Tabares (2021) and later integrating them into models of the urban system, such as that of Cortés Zambrano et al. (2020),

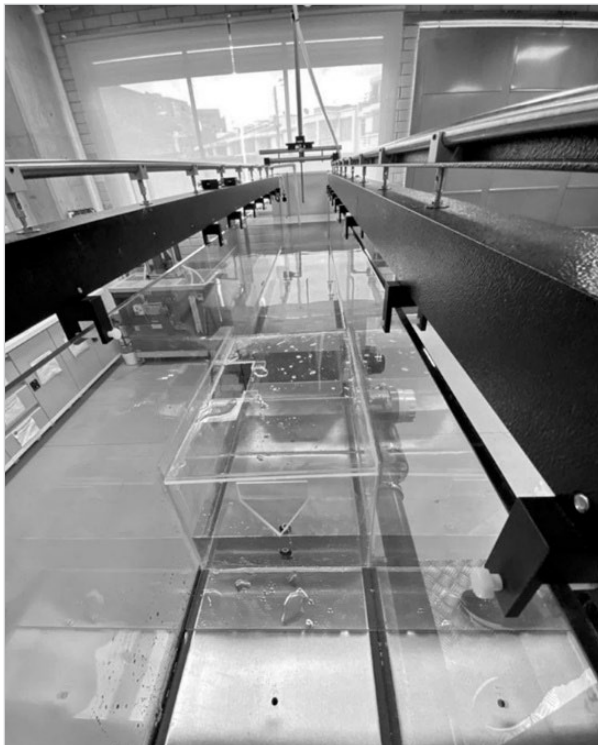
This study presents, in detail, the step-by-step advance for three-dimensional numerical research. It seeks to build robust and flexible models that capitalize on the advantages of CFD, including control over boundary conditions, attainment of data in different scales in specific points, and a full-scale study under different conditions. In addition, some of the results obtained are analyzed, discussed, and tested in order to make a statement of the usefulness, limitations, and improvement options for future studies, as recommended by Jakeman et al. (2006).

Experimental Development

Experimental campaign

This campaign was developed by Chaparro Andrade and Abaunza Tabares (2021), with a physical prototype on a reduced scale that represented a road lane that was 2.75-m wide and 4.0-m long. This can be seen in Fig. 1.

Fig. 1. Physical model of the experimental campaign (source: Chaparro Andrade and Abaunza Tabares, 2021)



The seven types of grate inlets shown in Fig. 2 were tested, varying the longitudinal slope between values of $S_L = 1.0, 1.5$ and 2.0% , keeping the transverse slope fixed at $S_L = 1.0$ and a flow rate Q_{Street} of 34.1 l/s .

These tests were carried out in a rectangular channel with a variable slope, measuring the intercepted flow with a triangular V-shaped weir and a limnimeter, in the Hydraulics laboratory of the Santo Tomás University (Tunja).

Numerical model

In order to verify the results of the physical experimental phase of prototypes, the experimental slope combinations were maintained, whilst the range of the volume of the test flow of water was expanded to $Q_{Street} = 24, 34.1, 44, 100, 200$ and 300 L/s , for a total of 126 models.

Table 1. Geometric characteristics of the typologies tested

N° Grade Type	Length (cm)	Width (cm)	Effective Area (m ²)	Area of Openings (m ²)	% Openings
Type 1	0.90	0.42	0.219	0.150	68.49
Type 2	0.65	0.42	0.221	0.160	72.56
Type 3	1.15	0.48	0.343	0.242	70.40
Type 4	0.72	0.38	0.205	0.126	61.54
Type 5	0.70	0.40	0.218	0.163	74.84
Type 6	1.00	0.40	0.317	0.163	51.52
Type 7	0.55	0.55	0.270	0.179	66.04

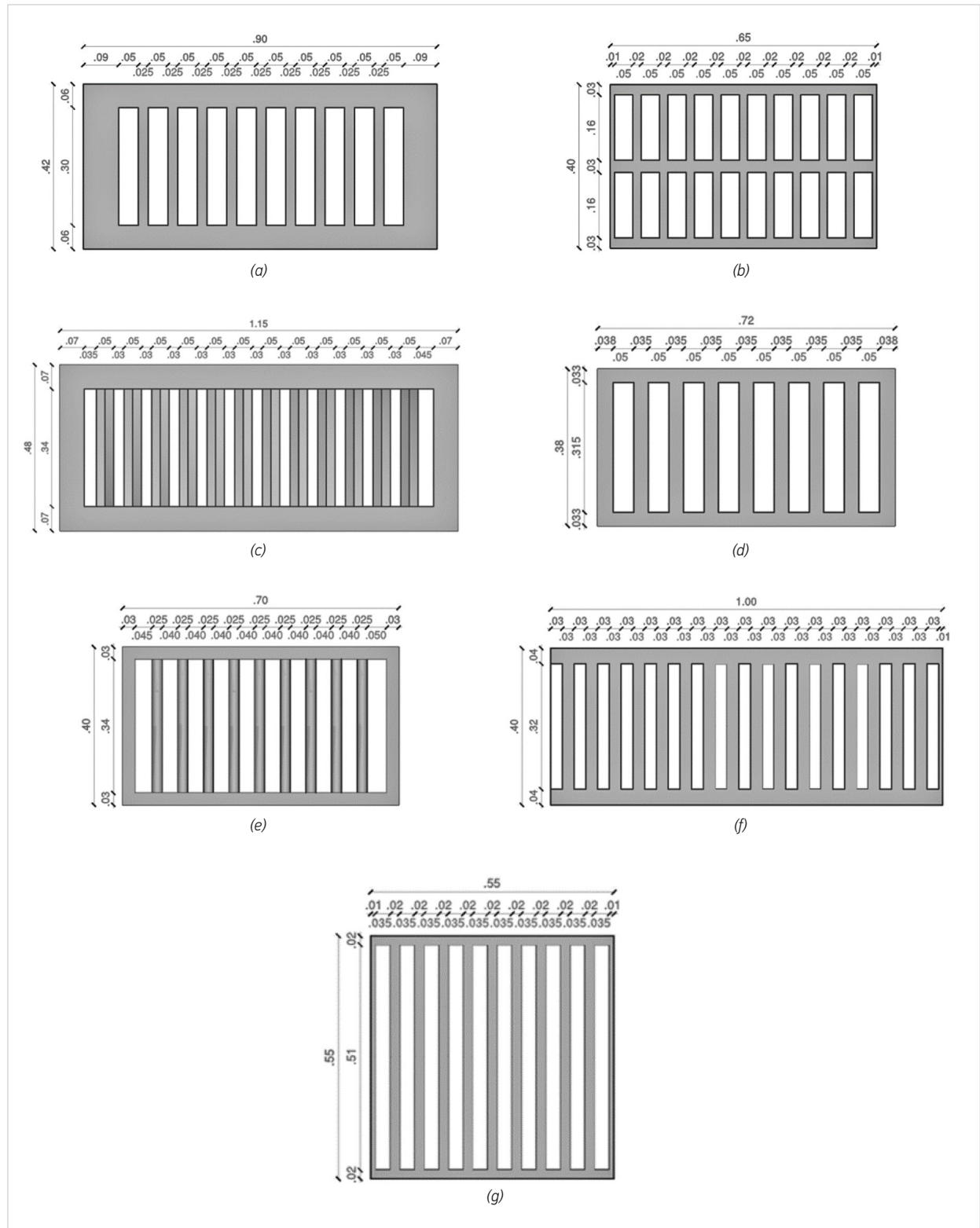
Mathematical formulation of the three-dimensional flow movement: The FLOW-3D® solver (Flow Science, 2019), a CFD 3D numerical model, was selected and used, taking into account the results obtained by Téllez Álvarez et al. (2003, 2017, 2019).

The numerical simulation was performed with the Reynolds averaged three-dimensional numerical approach for the Navier-Stokes equations (RANS), to solve the continuity and moment equations (Flow Science, 2018):

$$V_F \frac{\partial p}{\partial t} + \frac{\partial}{\partial x}(\rho u A_x) + R \frac{\partial}{\partial y}(\rho u A_y) + \frac{\partial}{\partial z}(\rho u A_z) + \xi \frac{\rho u A_x}{x} = R_{DIF} + R_{SOR} \quad (1)$$

Where: V_F is the fraction of volume open to flow, ρ is the density of the fluid, R_{DIF} is the turbulent diffusion, R_{SOR} is the source of mass. The velocity components (u, v, w) are in coordinate directions (x, y, z) or (r, R_{SOR}, z). A_x is the fractional area open to flow in the x direction, A_y and A_z are similar fractional areas open to flow in the y and z directions respectively.

Fig. 2. Design of the grate inlet types studied: (a) R1, (b) R2, (c) R3, (d) R4, (e) R5, (f) R6, (g) R7 (source: based on geometries of Chaparro Andrade and Abaunza Tabares, 2021)



The Navier-Stokes equations with some additional terms represent the motion in the three coordinate directions, as described by Equations (2), (3) and (4):

$$\frac{\partial u}{\partial t} + \frac{1}{V_F} \left\{ u A_x \frac{\partial u}{\partial x} + v A_y R \frac{\partial u}{\partial y} + w A_z \frac{\partial u}{\partial z} \right\} - \xi \frac{A_y v^2}{x V_F} = -\frac{1}{p} \frac{\partial p}{\partial x} + G_x + f_x - b_y - \frac{R_{SOR}}{p V_F} (u - u_w - \delta u_s) \quad (2)$$

$$\frac{\partial v}{\partial t} + \frac{1}{V_F} \left\{ u A_x \frac{\partial v}{\partial x} + v A_y R \frac{\partial v}{\partial y} + w A_z \frac{\partial v}{\partial z} \right\} + \xi \frac{A_y u v}{x V_F} = -\frac{1}{p} \left(R \frac{\partial p}{\partial x} \right) + G_y + f_y - b_y - \frac{R_{SOR}}{p V_F} (v - v_w - \delta v_s) \quad (3)$$

$$\frac{\partial w}{\partial t} + \frac{1}{V_F} \left\{ u A_x \frac{\partial w}{\partial x} + v A_y R \frac{\partial w}{\partial y} + w A_z \frac{\partial w}{\partial z} \right\} = -\frac{1}{p} \frac{\partial p}{\partial z} + G_z + f_z - b_z - \frac{R_{SOR}}{p V_F} (w - w_w - \delta w_s) \quad (4)$$

Where: G_x , G_y and G_z are body accelerations, f_x , f_y and f_z are viscous accelerations, b_x , b_y and b_z are flow losses in porous materials or through porous deflector plates, and the last terms consider the injection of mass in a source represented by a geometric component.

The term $u_w = (u_w, v_w, w_w)$ in equations (2), (3) and (4) is the velocity of the source component, which will generally not be zero for a mass source in a General Model of Moving Objects and $u_s = (u_s, v_s, w_s)$ is the velocity of the fluid at the surface of the source relative to the source itself.

The effect of gravity was defined in the z axis with the value of 9.81 m/s². This parameter was changed in the x and y direction for each configuration of the slope in the study, according to the longitudinal and transverse inclination of the platform.

Calculation domain. Geometries were generated in CAD software at a 1:1 scale. They were exported in the STereoLithography (STL) format, imported and then checked using the qAdmesh tool provided in the program.

Then a Cartesian coordinate system was defined, subdividing the domain into three structured meshes with cubic hexahedral elements: firstly, a general mesh with an element size of 0.02 m, which corresponds to the virtual platform; secondly, a mesh nested around each grid that maintained a 2:1 relationship (general:

detailed), in a volume of 2 m long by 1 m wide and 0.35 m high; and finally, a mesh adjacent to the nesting, which corresponds to the grate dimensions plus 0.05 cm on each side (width and length), with which the flow captured by the grate is determined.

Fig. 3. Subdivision of the domain in FLOW-3D®: general, nested in grid and sink outlet, inside the test platform (source: produced with FLOW-3D®)



Boundary conditions and other configurations. With respect to the boundaries, an input was established in terms of the fluid volume rate for $Q_{STREET} = 24, 34.1, 44, 100, 200$ and 300 L/s, specific pressure at atmospheric pressure, and two outputs, one for the flow captured by the bottom grate and another at the platform outlet, downstream of the grate.

In order to represent the initial condition of a platform full of air, a fluid fraction of zero was established with a depth of water sheet at the inlet, allowing it to be filled until the permanent state condition was achieved. The integration between water and air was considered in the simulations through the use of the VOF method for multiphase flows, facilitating the evaluation of the advection of the moment with first-order precision.

A roughness value of 0.3 mm was set for the platform, without distinguishing absolute roughness variation or change of gutter lane material. A uniform section of the slope and the finish was formed which restricted the flood width to a single pumping.

Turbulence models. In urban drainage, unstable, three-dimensional flow conditions are observed with randomness, implying turbulent flows. These conditions are related to frictional resistance, flow separation, transition from laminar to turbulent flow, extension of secondary flows, the propagation of jets

and contrails, and rapid flow variations (Vyzikas and Greaves, 2018). Given the conditions of depth of the water sheet, the hydraulic characteristics of the flow may have a greater influence on the shear stresses than the disturbances in the flow around the grates. This led to the selection of the turbulence model of the Renormalization group (RGN) (Yakhot and Orszag, 1986; Yakhot and Smith, 1992), which describes low intensity turbulent flows and flows that have strong shear regions with greater precision, implemented in FLOW-3D® (Flow Science, 2018).

In addition, it is the most commonly used method for free flow analysis, as well as the most stable one (Fang et al., 2010; Gómez Valentin, 2007; Jang et al., 2019; Kleidorfer et al., 2018; Téllez Álvarez et al., 2003).

Results and Discussion

Influence of mesh refinement on captured flows

With 15 seconds of simulation, convergence conditions of stable flow were achieved. As recommended by Jakeman et al. (2006), an analysis of the sensitivity to meshing changes was performed. The dimensions of the openings of each type of grate inlet and

the estimated depths of flow for stable flow conditions were taken into account. The summary of some results obtained is shown in *Table 2*.

For the simulations, two mesh sizes were defined: one of 0.02 m for the general or platform subdomain and 0.01 m for the nested subdomain (flow around the grid), one of flow output through the grid. There was a low variation in the results obtained. An optimal structured mesh size was sought according to the available computational resources and independence of the results, with respect to the mesh size used with a reasonable computation time. This coincided with the modelling experiences of Manuel Gómez et al. (2016), Cárdenas-Quintero et al. (2018) and Tellez-Alvarez et al. (2019).

Comparison of flow patterns with experimental campaign results

Figs. 4 and 5 present an example comparison of the results of the simulations for grate types 7 and 10. In these figures, the three-dimensional numerical simulation approach is evidenced. Some phenomena are reproduced, such as flow propagation, weir function, hydraulic overhang, and dry fronts. These were observed in the physical experimental campaign carried out by Chaparro Andrade and Abaunza Tabares (2021).

Table 2. Examples of results obtained from mesh sensitivity tests for some types

Mesh	Grate	S_x	S_L	\bar{U}	Q_{street}	Q_{out}	y	Esim
		(m/m)	(m/m)	(m/s)	(l/s)	(l/s)	(mm)	
0.02 m and 0.01 m	R3	0.01	0.02	0.66	24.1	11	25.88	0.456
0.01 m and 0.005 m				0.75	24	9.9	25.82	0.410
Relative Error								11.00%
0.02 m and 0.01 m	R7	0.01	0.01	0.97	100	24.3	55.52	0.243
0.01 m and 0.005 m				0.96	100	23.6	56.69	0.234
Relative Error								3.00%
0.02 m and 0.01 m	R4	0.01	0.02	1.49	299.9	46.9	88.32	0.156
0.01 m and 0.005 m				1.49	300	43.8	88.84	0.146
Relative Error								7.00%

Fig. 4. Comparison between the results obtained during physical experimentation in prototype 7 and simulation results with FLOW-3D® (source: made with FlowSight® and photographic record by Chaparro Andrade and Abaunza Tabares, 2021)

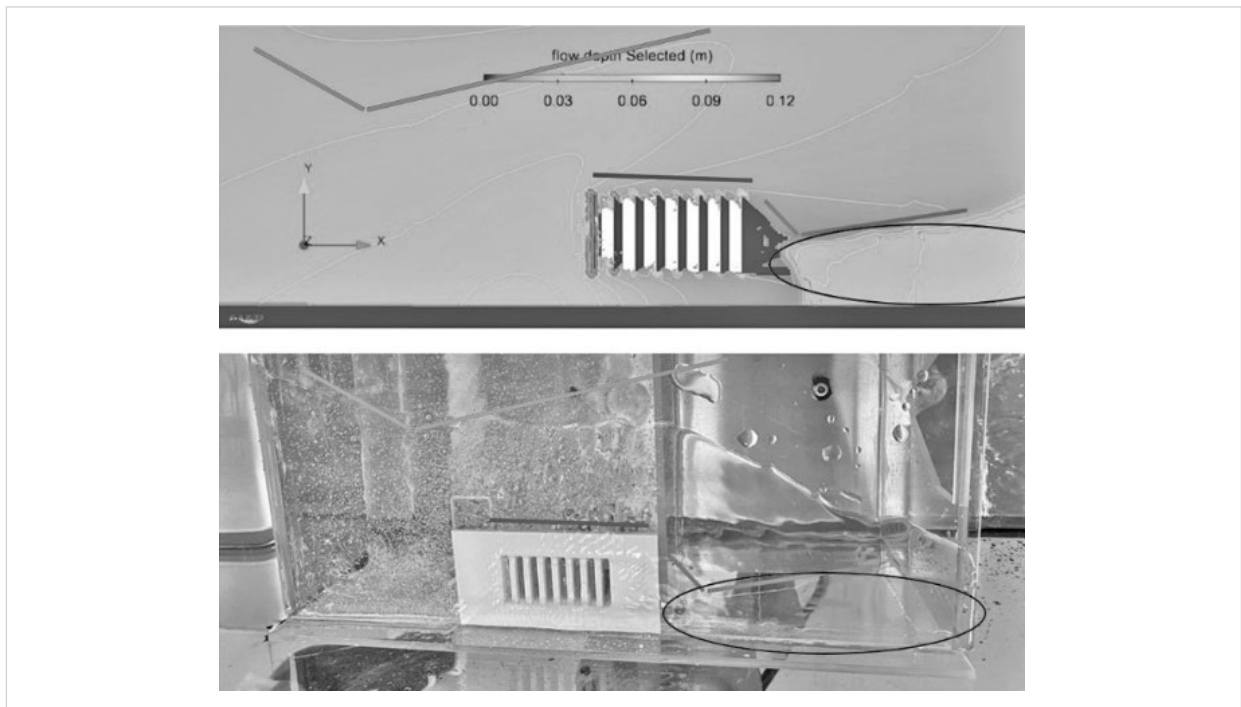


Fig. 5. Comparison between results obtained during physical experimentation in prototype 10 and simulation results with FLOW-3D® (source: made with FlowSight® and photographic record by Chaparro Andrade and Abaunza Tabares, 2021)

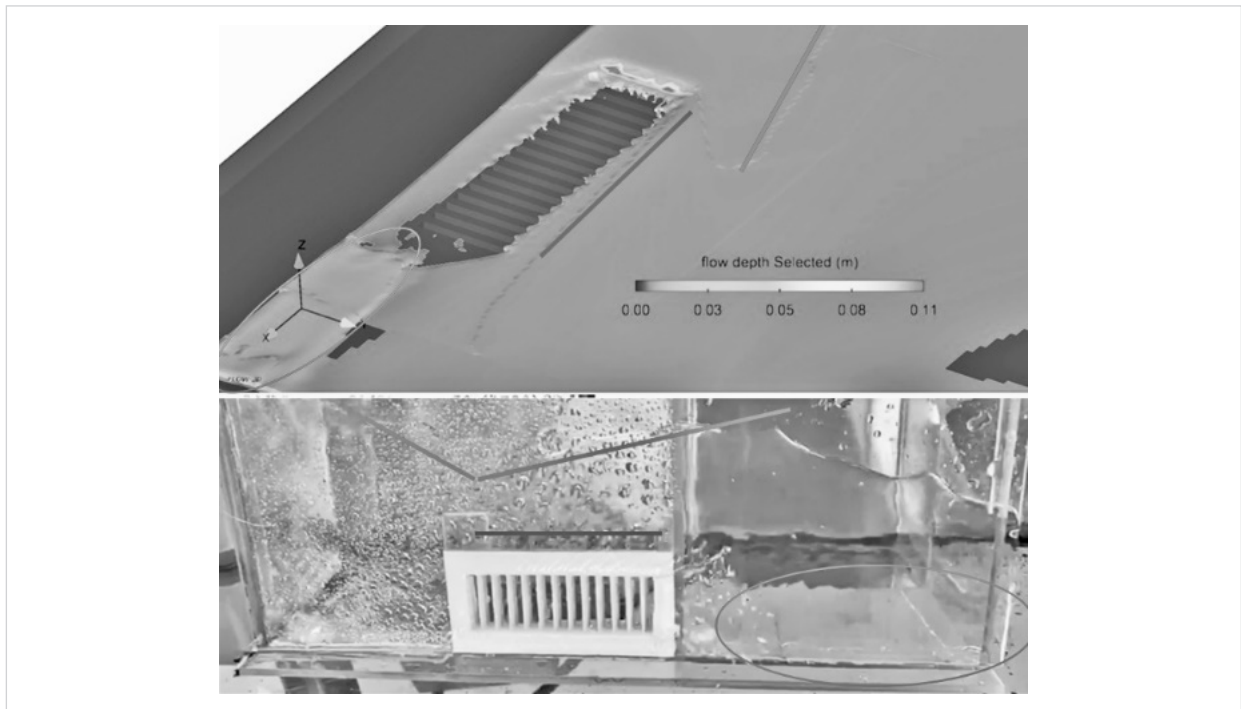
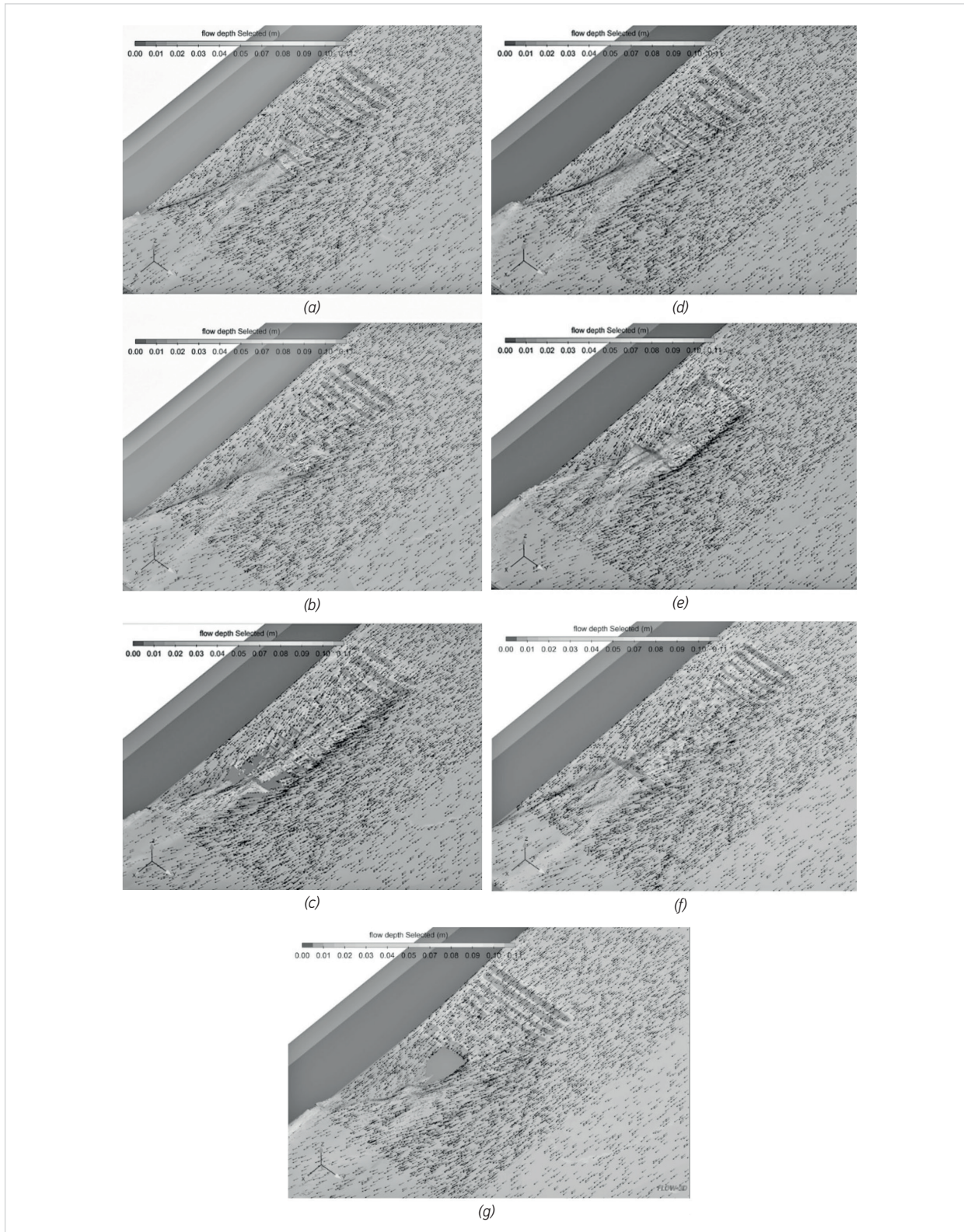


Fig. 6. Example of the results of flow depth and velocity vectors in the xy plane, for a stable flow condition in a grate inlet type and free surface configuration and flow regime, of some grating types (source: produced with FlowSight®)



Sheet depth and velocity pattern

The results of the simulations show the two-dimensional flow patterns in the sectors of the grate and their surroundings. In some cases, dry fronts are observed until the middle of the grid, reaching partial and total submergence conditions for some experimental combinations.

In all test cases, a pattern was noted in which the depth of the sheet increased when the water flow increased and the slope decreased. Upstream of the grate, the generation of a hydraulic projection behind the dry front, repels, in some cases, with an increase in the longitudinal slope, and in other cases over the grate.

The two-dimensional lateral propagation of the excess flow of water that flows without being captured by the grid is observed, extending from the curb in the vicinity of the first intake opening. In most of the cases evaluated, the lateral extension but not the concentration of the flow, occupies the entire test lane in the vicinity of the curb. This is preserved with the change in longitudinal slope and is partial for flows of 24 L/s.

Comparison of results with other investigations

To compare the catchment capacity of the different types of grating, longitudinal slopes and test flows, the inlet efficiency related to a lane with longitudinal and transverse slope (E') was evaluated. The definition of catchment proficiency provided by Despotovic et al. (2005) was used:

$$E' = \frac{Q_{out}}{Q_{street}} \quad (5)$$

For each type of the grate inlet tested, hydraulic inlet efficiency curves were constructed for each of the test longitudinal slope configurations, as a function of the street flow ratio – flow depth measured at the curb (Q/Y).

The catchment hydraulic efficiency curves versus the flow rate-flow depth ratio are better adjusted (according to the coefficient of determination) to a decreasing potential function (hyperbola), with a negative exponent and a positive coefficient. This coincides with that reported by Cárdenas-Quintero et al. (2018), Gómez and Russo (2011), Gómez Valentin (2007).

The results were then compared with the formulations proposed by the Polytechnic University of Catalonia

and the University of Zaragoza, in order to verify the results obtained with reference studies. The proposed methodologies are based on the studies carried out by Spaliviero et al. (2000) and relate the total efficiency of the grate inlet with the Q/y relationship through a potential function, where the coefficients A and B vary for each particular typology and can be calculated based on the geometric characteristics of the grids, without previous experimental tests (Gómez and Russo, 2005b). This is described in Equation (6). This has been adjusted to a road width of 2.75 m. For the present study, the formulations made by Gómez and Russo (2005a) and Gómez and Russo (2011) have been evaluated, and are described in Equations (7), (8), (9) and (10).

$$E' = A \left(\frac{Q}{Y} \right)^{-B} \quad (6)$$

$$A = \frac{0.39}{A_g^{0.35} \cdot p^{-0.13}} (n_t + 1)^{0.01} (n_l + 1)^{0.11} (n_d + 1)^{0.03} \quad (7)$$

$$B = 0.36 \frac{L}{W} \quad (8)$$

$$A = \frac{1.988 \cdot A_g^{0.403}}{p^{0.19} (n_t + 1)^{0.088} (n_l + 1)^{0.012} (n_d + 1)^{0.082}} \quad (9)$$

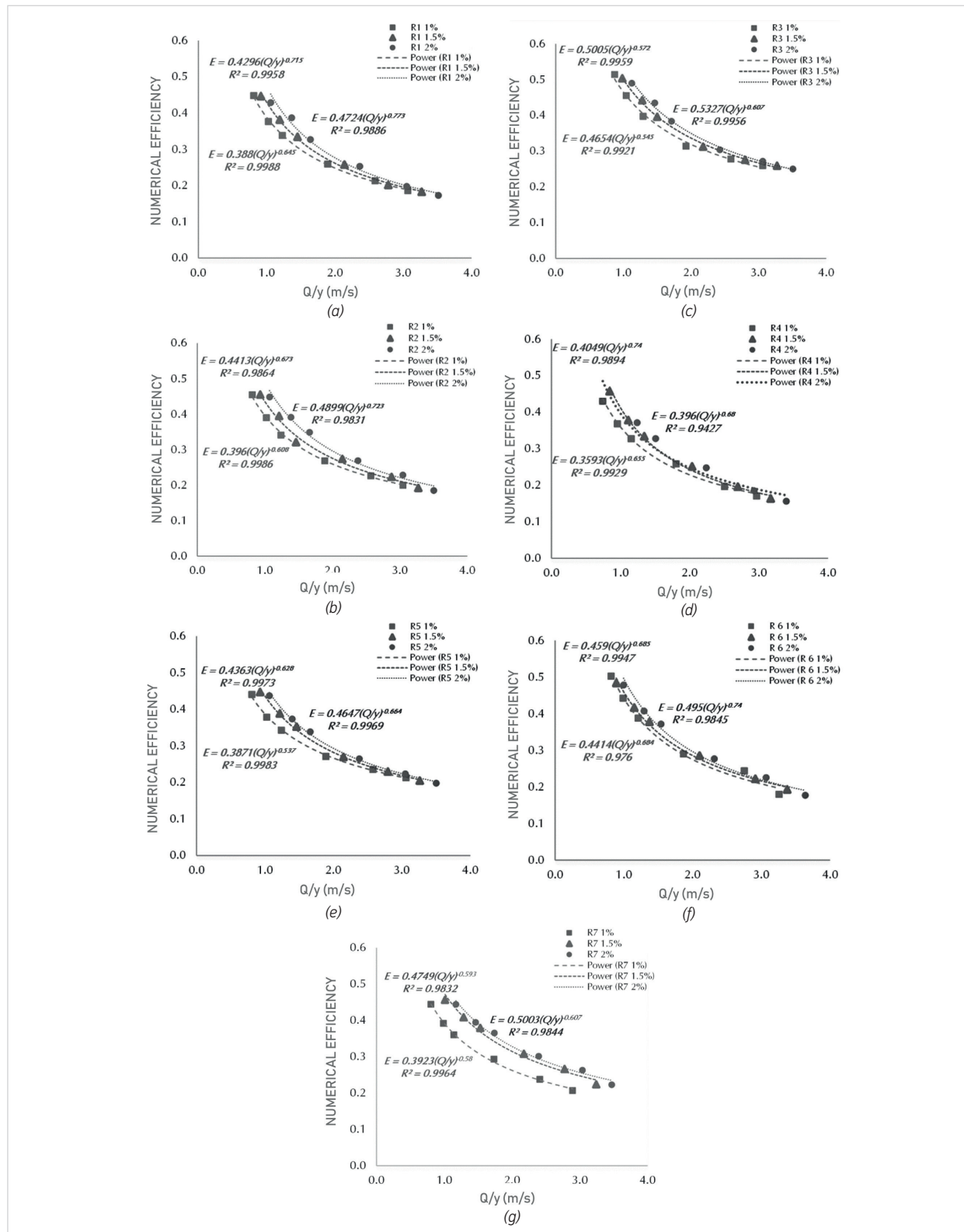
$$B = 1.346 \frac{L^{0.179}}{W^{0.394}} \quad (10)$$

Where: E is the inlet efficiency, Q is the total discharge approaching the inlet (m^3/s), Y is the flow depth (m), A and B are two characteristic coefficients of the grate and specifically can be expressed in terms of geometrical data of the grate inlet, n_t number of transversal bars, n_l number of longitudinal bars, n_d number of diagonal bars, A_g is the area that encompasses all the holes in the grid or clear area of opening, p is the percentage of gaps area, L is the grate length, W is the grate width.

Graphs were generated with the obtained results, with error limits of +20.1% and -46.0% (maximum positive and maximum negative) and -35.6% (maximum negative). These results are then compared with those proposed by Gómez and Russo (2005a) and Gómez and Russo (2011).

There is less relative deviation between the results of the formulation proposed by Gómez and Russo (2011)

Fig. 7. Inlet efficiency curves obtained for the tested gates: (a) R1, (b) R2, (c) R3, (d) R4, (e) R5, (f) R6, (g) R7 (source: study)



compared to that made by Gómez and Russo (2005a), with maximum negative relative errors of 35.6% versus -46%, tending to be in high flow values. In addition, the results obtained show a positive correlation, with $R^2 = 0.98, 0.98, 0.99, 0.98, 0.98, 0.99, 0.94$, for the types of grate inlets tested, 1, 2, 3, 4, 5, 6 and 7.

Fig. 8. Relative deviations between the numerical results and the proposal of Gómez and Russo (2005a) (source: study)

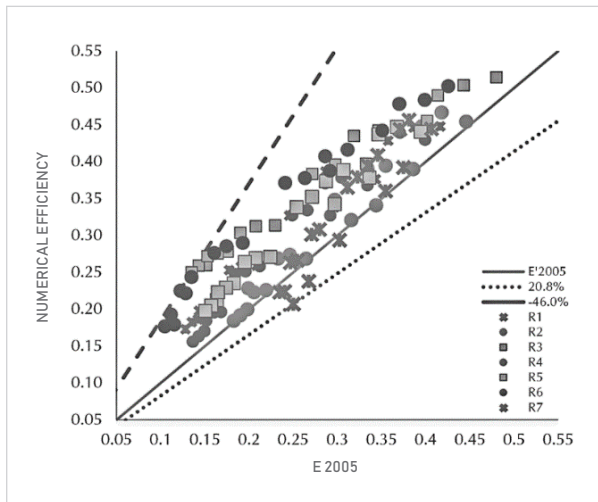
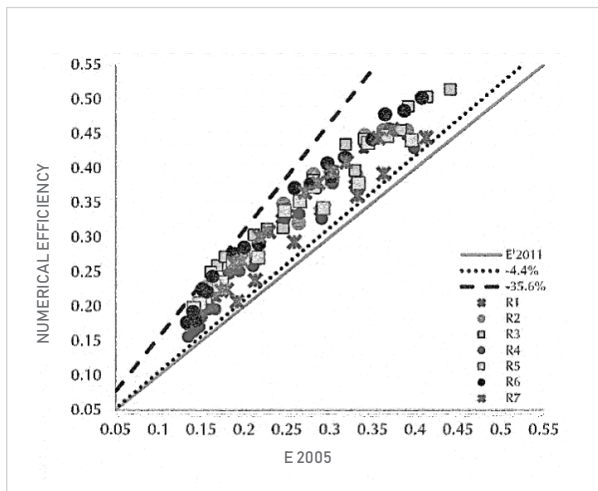


Fig. 9. Relative deviations between the numerical results and the proposal of Gómez and Russo (2011) (source: study)



Orifice type discharge coefficient

In order to analyze the discharge coefficient (C_d), the formula of an orifice was used:

$$C_d = \frac{Q_{cap}}{A_g \sqrt{2 \cdot g \cdot \Delta h}} \tag{11}$$

Where: Q_{cap} is captured flow, A_g the area of holes in the grid, Δh is the water level above the level of the bottom grid upstream of it, and g is the acceleration of gravity.

This was done in order to estimate discharge coefficient values to be compared later in real-scale physical experimental campaigns. Figs. 10a, 10b, 10c, 10d, 10e, 10f and 10g present the summary graphs of the results obtained by type of grate for each value of longitudinal slope.

The discharge coefficient results obtained from three-dimensional numerical experimentation show a range of values between 0.07 and 0.39, for volumetric flow rates captured between 9.9 L/s and 77.9 L/s.

Results verification of physical experimentation of prototypes

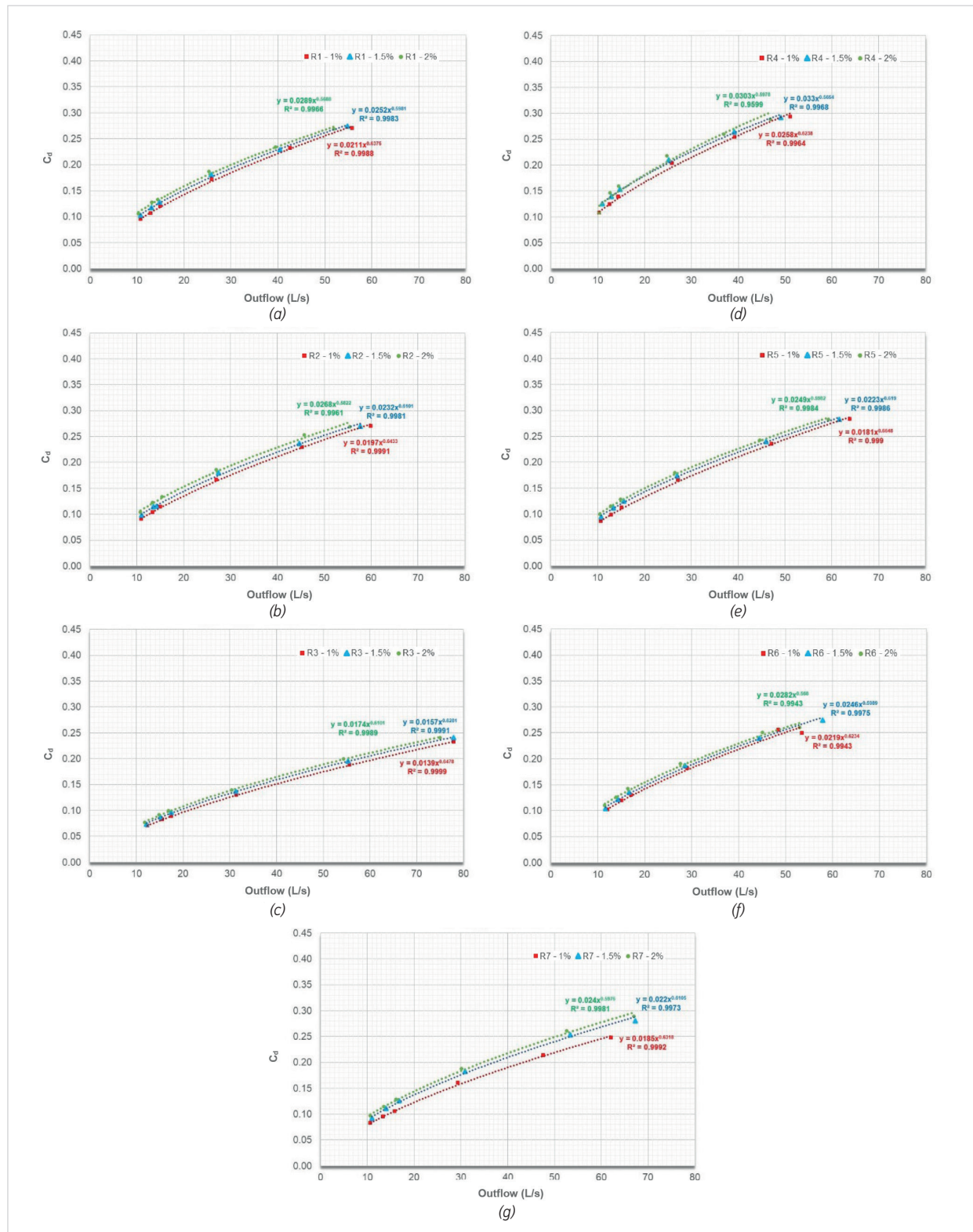
Once the collection efficiency values of the evaluated grates were obtained, the results obtained from the simulation were compared with those reported by Chaparro Andrade and Abaunza Tabares (2021).

Significant differences were found, registering discrepancies of up to 0.27 in the collection efficiency values, equivalent to relative errors of 72.3%. This can be explained by the difficulty in representing transitions from the flow to the turbulent flow and turbulence phenomena to the scale used, and that were evidenced in the numerical modelling.

Table 3. Comparison of efficiency results obtained through numerical modelling and experimentation with prototypes, for a longitudinal slope of 1.5%

Grate InletType	Numerical Inlet Efficiency	Inlet Efficiency of Experimental Prototypes	Relative Error
R1	0.38	0.60	56.9%
R2	0.39	0.59	50.3%
R3	0.44	0.62	39.3%
R4	0.38	0.65	72.3%
R5	0.39	0.54	38.4%
R6	0.42	0.67	60.9%
R7	0.41	0.68	67.0%

Fig. 10. Orifice type discharge coefficient curves for the grates tested: (a) R1, (b) R2, (c) R3, (d) R4, (e) R5, (f) R6, (g) R7 (source: study)



This has already been reported by Argue and Pezzaniti (1996), who mentioned the implications of applying simple Froude's law scale relationships to triangular flow cases and recommended the exclusive use of full-scale experimentation platforms.

In addition to the implications for the dimensions of the grate inlet, there are further considerations. The effects of the reduction of the scale, the operation of the implemented instrumentation, the errors that can be induced in the precision of the measurements and other factors may have been overlooked or ignored, but are a source of uncertainty.

Conclusions

A numerical approach was formulated and implemented for the evaluation of hydraulic efficiency of grate inlets of drains. Seven different types of grate inlet that are usually found in the city of Tunja were analyzed through the construction of models and use of CFD-3D simulations with VOF-type elements in a commercial software.

Comparison of the obtained results with the formulas proposed by the Universidad Politécnica de Cataluña and the Universidad de Zaragoza allowed us to demonstrate the capacity of the three-dimensional numerical simulation in the study of capture methods. Maximum relative deviations of -39.3% were achieved, which evidences a better fit with the methodology proposed by Gómez and Russo (2011), one of the most robust formulations proposed to date (Alia Md. and Sabtu, 2020).

The inlet efficiency of the grate inlets does not correspond to a single value and is a function of the hydraulic characteristics of the street flow (speed, sheet depth, flood width, and specific energy), the grate geometry, its location on the road, and the longitudinal slope of the drainage surface.

The 3D CFD simulation for a wide range of flows and longitudinal street slopes allowed the construction of inlet efficiency curves and also the orifice-type discharge coefficient curves for the different types of bottom side grates studied. In addition, the qualitative understanding of the flow characteristics in these collection elements was also described for the following: two-dimensional flow patterns in the grate,

functioning as a lateral and frontal weir in some areas of the grate, recirculation areas of the flow, areas of projections, dry fronts, flow propagation and orifice-type operating conditions, and in cases of partial or total submergence of the grid intake openings.

The differences found in the catchment values and results of the hydraulic inlet efficiency and the discharge coefficient of grate inlet types 2, 4 and 11 demonstrated the influence of the definition of an adequate mesh size of the domain. This served to highlight the importance of building models that reproduce flow conditions with convergence or results, independent of meshing; avoiding leading to discrepancies that may limit the replication of the results.

The results showed that for the experimental combinations of single pumping of 1.0% and longitudinal slope of 1.0% , 1.5% and 2.0% , no type of grate inlet presents 100% collection efficiency for the test lane flows (24, 34.1, 44, 100, 200 and 300 L/s). In all cases, the remaining flow and bidirectional propagation of this non-captured flow were configured.

The results of the 3D CFD simulation made it possible to verify the results of the physical experimentation of prototypes. When these results were compared with those derived from the physical simulation, significant discrepancies in the collection efficiency values obtained through prototypes were evidenced.

The achievement of partial and total submergence conditions in the hydraulic evaluation of the catchment of the seven types of grids evidences the importance of continuing to study the hydraulics in these catchment elements, in order to obtain the definition of the equations to be used for efficiencies less than 90% . Given the need to evaluate the existing catchment elements in the already consolidated urban context, it may be possible to support intervention plans that seek the rehabilitation, correction, and improvement of the existing draining system and its associated problems.

The present work has made it possible to determine a series of values and build discharge coefficient curves for each of the grids studied. The different combinations of configurations will be able to be compared in future real-scale physical experimental campaigns, allowing for the results reported here to be supported.

Although the present work has confirmed the abilities of 3D CFD hydraulic modelling and recognized

its usefulness as a tool with which we can study and understand hydraulic operation, further research in real-scale physical tests is required.

Acknowledgements

We would like to thank Flow3D Latinoamérica for granting us the research software license which

afforded us the possibility to conduct the simulations presented in this study. The authors would like to acknowledge the support of the Seedbed for Research in Sustainable Management of Materials and Hydro-Environmental Resources (MSMRHA) of the Santo Tomás University.

References

- Alia Md., S., and Sabtu, N. (2020). Comparison of Different Methodologies for Determining the Efficiency of Gully Inlets. In F. M. Nazri (Ed.), *Proceedings of AICCE'19: Transforming the Nation for a Sustainable Tomorrow* (Vol. 53, pp. 1275-1284). Springer Nature Switzerland AG. https://doi.org/10.1007/978-3-030-32816-0_99
- Antunes do Carmo, J. S. (2020). Physical Modelling vs. Numerical Modelling: Complementarity and Learning. July. <https://doi.org/10.20944/preprints202007.0753.v1>
- Aragón-Hernández, J. L. (2013). Modelación numérica integrada de los procesos hidráulicos en el drenaje urbano [Universidad Politécnica de Cataluña]. In *Doctoral Tesis*. <https://upcommons.upc.edu/handle/2117/95059?locale-attribute=es>
- Argue, J. R., and Pezzaniti, D. (1996). How reliable are inlet (hydraulic) models at representing stormwater flow? *Science of the Total Environment*, 189-190, 355-359. [https://doi.org/10.1016/0048-9697\(96\)05231-X](https://doi.org/10.1016/0048-9697(96)05231-X)
- Banco Mundial, O. (2019). Agua: Panorama general. <https://www.bancomundial.org/es/topic/water/overview>
- Cárdenas-Quintero, M., Carvajal-Serna, L. F., and Marbello-Pérez, R. (2018). Evaluación numérica tridimensional de un sumidero de reja de fondo (Three-Dimensional Numerical Assessment of Grate Inlet). *SSRN Electronic Journal*, November. <https://doi.org/10.2139/ssrn.3112980>
- Carvalho, R. F., Lopes, P., Leandro, J., and David, L. M. (2019). Numerical Research of Flows into Gullies with Different Outlet Locations. *Water*, 11(2), 794. <https://doi.org/10.3390/w11040794>
- Chaparro Andrade, F. G., and Abaunza Tabares, K. V. (2021). Importancia de los sumideros, su funcionamiento y diseño en redes de alcantarillado caso de estudio sector nororiental Tunja. *Universidad Santo Tomás*.
- Cortés Zambrano, M., Amaya Tequia, W. E., and Gamba Fernández, D. S. (2020). Implementation of the hydraulic modelling of urban drainage in the northeast sector, Tunja, Boyacá. *Revista Facultad de Ingeniería Universidad de Antioquia*. <https://doi.org/10.17533/udea.redin.20200578>
- Cosco, C., Gómez, M., Russo, B., Tellez-Alvarez, J., Macchiome, F., Costabile, P., and Costanzo, C. (2020). Discharge coefficients for specific grated inlets. Influence of the Froude number. *Urban Water Journal*, 17(7), 656-668. <https://doi.org/10.1080/1573062X.2020.1811881>
- Despotovic, J., Plavsic, J., Stefanovic, N., and Pavlovic, D. (2005). Inefficiency of storm water inlets as a source of urban floods. *Water Science and Technology*, 51(2), 139-145. <https://doi.org/10.2166/wst.2005.0041>
- Ellis, J. B., and Marsalek, J. (1996). Overview of urban drainage: Environmental impacts and concerns, means of mitigation and implementation policies. *Journal of Hydraulic Research*, 34(6), 723-732. <https://doi.org/10.1080/00221689609498446>
- Fang, X., Jiang, S., and Alam, S. R. (2010). Numerical simulations of efficiency of curb-opening inlets. *Journal of Hydraulic Engineering*, 136(1), 62-66. [https://doi.org/10.1061/\(ASCE\)HY.1943-7900.0000131](https://doi.org/10.1061/(ASCE)HY.1943-7900.0000131)
- Faram, M. G., and Harwood, R. (2000). CFD for the Water Industry; The Role of CFD as a Tool for the Development of Wastewater Treatment Systems. *Hydro International*, 21-22.
- Faram, M. G., and Harwood, R. (2002). Assessment of the effectiveness of stormwater treatment chambers using computational fluid dynamics. *Global Solutions for Urban Drainage*, 40644(September 2002), 1-14. [https://doi.org/10.1061/40644\(2002\)7](https://doi.org/10.1061/40644(2002)7)
- Flow Science, I. (2018). FLOW-3D® Version 12.0 Users Manual. In FLOW-3D [Computer software]. <https://www.flow3d.com>
- Flow Science, I. (2019). FLOW-3D® Version 12.0 [Computer software] (No. 12). <https://www.flow3d.com>
- Ghanbari, R., and Heidarnajad, M. (2020). Experimental and numerical analysis of flow hydraulics in triangular and rectangular piano key weirs. *Water Science*, 00(00), 1-7. <https://doi.org/10.1080/11104929.2020.1724649>

- Gómez, M., and Russo, B. (2005a). Comparative study of methodologies to determine inlet efficiency from test data. HEC-12 methodology vs UPC method. *Water Resources Management*, Algarve, Portugal, 80(October 2014), 623-632. <https://doi.org/10.2495/WRM050621>
- Gómez, M., and Russo, B. (2005b). Comparative study among different methodologies to determine storm sewer inlet efficiency from test data. 10th International Conference on Urban Drainage, August, 21-26. https://www.researchgate.net/publication/255602448_Comparative_study_among_different_methodologies_to_determine_storm_sewer_inlet_efficiency_from_test_data
- Gómez, M., Recasens, J., Russo, B., and Martínez-Gomariz, E. (2016). Assessment of inlet efficiency through a 3D simulation: Numerical and experimental comparison. *Water Science and Technology*, 74(8), 1926-1935. <https://doi.org/10.2166/wst.2016.326>
- Gómez, M., and Russo, B. (2011). Methodology to estimate hydraulic efficiency of drain inlets. *Proceedings of the Institution of Civil Engineers: Water Management*, 164(2), 81-90. <https://doi.org/10.1680/wama.900070>
- Gómez Valentin, M. (2007). Hidrología urbana. In *Hidrología Urbana* (pp. 135-147). Instituto Flumen.
- Jakeman, A. J., Letcher, R. A., and Norton, J. P. (2006). Ten iterative steps in development and evaluation of environmental models. *Environmental Modelling and Software*, 21, 602-614. <https://doi.org/10.1016/j.envsoft.2006.01.004>
- Jang, J. H., Hsieh, C. T., and Chang, T. H. (2019). The importance of gully flow modelling to urban flood simulation. *Urban Water Journal*, 16(5), 377-388. <https://doi.org/10.1080/1573062X.2019.1669198>
- Kaushal, D. R., Thinglas, T., Tomita, Y., Kuchii, S., and Tsukamoto, H. (2012). Experimental investigation on optimization of invert trap configuration for sewer solid management. *Powder Technology*, 215-216, 1-14. <https://doi.org/10.1016/j.powtec.2011.08.029>
- Khazaei, I., and Mohammadiun, M. (2010). Effects of flow field on open channel flow properties using numerical investigation and experimental comparison. *International Journal of Energy and Environment*, 1(6), 1083-1096. [https://doi.org/10.1016/S0031-9384\(10\)00122-8](https://doi.org/10.1016/S0031-9384(10)00122-8)
- Kleidorfer, M., Tscheikner-Gratl, F., Vonach, T., and Rauch, W. (2018). What can we learn from a 500-year event? Experiences from urban drainage in Austria. *Water Science and Technology*, 77(8), 2146-2154. <https://doi.org/10.2166/wst.2018.138>
- Leitão, J. P., Simões, N. E., Pina, R. D., Ochoa-Rodríguez, S., Onof, C., and Sá Marques, A. (2017). Stochastic evaluation of the impact of sewer inlets' hydraulic capacity on urban pluvial flooding. *Stochastic Environmental Research and Risk Assessment*, 31(8), 1907-1922. <https://doi.org/10.1007/s00477-016-1283-x>
- Lopes, P., Leandro, J., Carvalho, R. F., Russo, B., and Gómez, M. (2016). Assessment of the ability of a volume of fluid model to reproduce the efficiency of a continuous transverse gully with grate. *Journal of Irrigation and Drainage Engineering*, 142(10), 1-9. [https://doi.org/10.1061/\(ASCE\)IR.1943-4774.0001058](https://doi.org/10.1061/(ASCE)IR.1943-4774.0001058)
- Mohsin, M., and Kaushal, D. R. (2016). 3D CFD validation of invert trap efficiency for sewer solid management using VOF model. *Water Science and Engineering*, 9(2), 106-114. <https://doi.org/10.1016/j.wse.2016.06.006>
- Palla, A., Colli, M., Candela, A., Aronica, G. T., and Lanza, L. G. (2018). Pluvial flooding in urban areas: the role of surface drainage efficiency. *Journal of Flood Risk Management*, 11, S663-S676. <https://doi.org/10.1111/jfr3.12246>
- Russo, B. (2010). Design of surface drainage systems according to hazard criteria related to flooding of urban areas [Universitat Politècnica de Catalunya]. <https://dialnet.unirioja.es/servlet/tesis?codigo=258828>
- Sedano-Cruz, K., Carvajal-Escoar, Y., and Ávila Díaz, A. J. (2013). ANÁLISIS DE ASPECTOS QUE INCREMENTAN EL RIESGO DE INUNDACIONES EN COLOMBIA. *Luna Azul*, 37, 219-218. <https://www.redalyc.org/articulo.oa?id=321729206014>
- Spaliviero, F., May, R. W. P., Escarameia, M. (2000). Spacing of road gullies. Hydraulic performance of BS EN 124 gully gratings. *HR Walingford*, 44(0). <https://doi.org/10.13140/RG.2.1.1344.0889>
- Téllez-Álvarez, J., Gómez, M., and Russo, B. (2020). Quantification of energy loss in two grated inlets under pressure. *Water (Switzerland)*, 12(6). <https://doi.org/10.3390/w12061601>
- Téllez Álvarez, J., Gómez, V., Russo, B., and Redondo, J. M. (2003). Performance assessment of numerical modelling for hydraulic efficiency of a grated inlet. 1, 6-8. <https://doi.org/10.16309/j.cnki.issn.1007-1776.2003.03.004>
- Téllez Álvarez, J., Gómez Valentin, M., Painedelli, A., and Russo, B. (2017). ACTIVIDAD EXPERIMENTAL DE I+D+i EN INGENIERÍA HIDRÁULICA EN ESPAÑA. In L. J. Balairón Pérez and D. López Gómez (Eds.), *Seminario 2017, Comunicaciones de las líneas prioritarias* (pp. 41-43). Universitat Politècnica de València. <https://doi.org/10.1017/CBO9781107415324.004>
- Téllez Álvarez, J., Gómez Valentin, M., and Russo, B. (2019). Modelling of Surge Flow Through Grated Inlet. In P. Gourbesville and G. Caignaert (Eds.), *Advances in Hydroinformatics*

cs. Springer, Singapore. <https://doi.org/10.1007/978-981-4451-42-0>

UNDRR, I., and CRED, I. (2018). *Pérdidas económicas, pobreza y Desastres 1998 - 2017* (Vol. 6, Issue 1). <https://doi.org/10.12962/j23373520.v6i1.22451>

Vyzikas, T., and Greaves, D. (2018). Numerical Modelling. In D. Greaves and G. Iglesias (Eds.), *Wave and Tidal Energy* (pp. 289-363). John Wiley and Sons Ltd. <https://doi.org/10.1002/9781119014492>

Yakhot, V., and Orszag, S. A. (1986). Renormalization Group Ana-

lysis of Turbulence. I . Basic Theory. *Journal of Scientific Computing*, 1(1), 3-51. <https://doi.org/10.1007/BF01061452>

Yakhot, V., and Smith, L. M. (1992). The renormalization group, the ϵ -expansion and derivation of turbulence models. *Journal of Scientific Computing*, 7(1), 35-61. <https://doi.org/10.1007/BF01060210>

Yazdanfar, Z., and Sharma, A. (2015). Urban drainage system planning and design - Challenges with climate change and urbanization: A review. *Water Science and Technology*, 72(2), 165-179. <https://doi.org/10.2166/wst.2015.207>



This article is an Open Access article distributed under the terms and conditions of the Creative Commons Attribution 4.0 (CC BY 4.0) License (<http://creativecommons.org/licenses/by/4.0/>).